FibeRobo: Fabricating 4D Fiber Interfaces by Continuous Drawing of Temperature Tunable Liquid Crystal Elastomers

Jack Forman
MIT Media Lab & MIT's Center for Bits and Atoms, Massachusetts Institute of Technology
jackform@mit.edu

Ozgun Kilic Afsar
MIT Media Lab, Massachusetts Institute of Technology
ozgun@mit.edu

Sarah Nicita
MIT Media Lab, Massachusetts Institute of Technology
sarahnic@mit.edu

Rosalie Hsin-Ju Lin
MIT Media Lab, Massachusetts Institute of Technology
hsinjuli@mit.edu

Liu Yang
MIT Media Lab, Massachusetts Institute of Technology
yang0219@mit.edu

Megan Hofmann
Khoury College of Computer Sciences, Northeastern University
m.hofmann@northeastern.edu

Akshay Kothakonda
MIT Media Lab, Massachusetts Institute of Technology
akshayk@mit.edu

Zachary Gordon
MIT Media Lab, Massachusetts Institute of Technology
gordo505@mit.edu

Cedric Honnet
MIT Media Lab, Massachusetts Institute of Technology
honnet@mit.edu

Kristen Dorsey
Electrical and Computer Engineering, Northeastern University
k.dorsey@northeastern.edu

Neil Gershenfeld
MIT's Center for Bits and Atoms, Massachusetts Institute of Technology
neilg@mit.edu

Hiroshi Ishii
MIT Media Lab, Massachusetts Institute of Technology
ishii@mit.edu

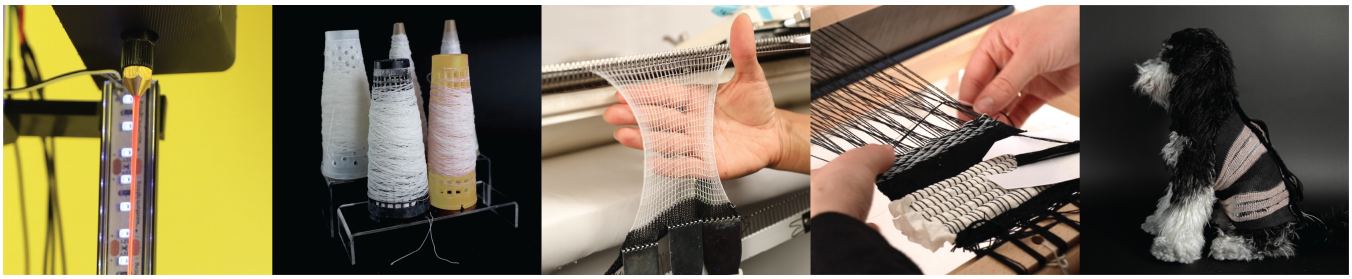

Figure 1: Pipeline from actuating fibers to 4D fabrics. From left to right, 1) FibeRobo being produced in a custom UV drawing machine, 2) 750m of fiber produced in a day, 3) machine knitting with FibeRobo, 4) weaving with FibeRobo, 5) a telepresence canine compression jacket.

ABSTRACT

We present FibeRobo, a thermally-actuated liquid crystal elastomer (LCE) fiber that can be embedded or structured into textiles and enable silent and responsive interactions with shape-changing, fiber-based interfaces. Three definitive properties distinguish FibeRobo from other actuating threads explored in HCI. First, they exhibit rapid thermal self-reversing actuation with large displacements (~40%) without twisting. Second, we present a reproducible UV fiber drawing setup that produces hundreds of meters of fiber with a sub-millimeter diameter. Third, FibeRobo is fully compatible with existing textile manufacturing machinery such as weaving looms, embroidery, and industrial knitting machines. This paper contributes to developing temperature-responsive LCE fibers, a facile and scalable fabrication pipeline with optional heating element integration for digital control, mechanical characterization, and the establishment of higher hierarchical textile structures and design space. Finally, we introduce a set of demonstrations that illustrate the design space FibeRobo enables.

UIST '23, October 29–November 01, 2023, San Francisco, CA, USA

ACM ISBN 979-8-4007-0132-0/23/10.
https://doi.org/10.1145/3586183.3606732

CCS CONCEPTS

• **Human-centered computing** → Human computer interaction (HCI); Interactive systems and tools.

KEYWORDS

morphing textiles, liquid crystal elastomer, shape-changing interfaces, maker culture, tangible

ACM Reference Format:
Jack Forman, Ozgun Kilic Afsar, Sarah Nicita, Rosalie Hsin-Ju Lin, Liu Yang, Megan Hofmann, Akshay Kothakonda, Zachary Gordon, Cedric Honnet, Kristen Dorsey, Neil Gershenfeld, and Hiroshi Ishii. 2023. FibeRobo: Fabricating 4D Fiber Interfaces by Continuous Drawing of Temperature Tunable Liquid Crystal Elastomers. In *The 36th Annual ACM Symposium on User Interface Software and Technology (UIST '23), October 29–November 01, 2023, San Francisco, CA, USA.* ACM, New York, NY, USA, 17 pages. https://doi.org/10.1145/3586183.3606732

1 INTRODUCTION

Researchers in HCI have grown increasingly interested in actuating fiber and fabrics as a medium for interactive surfaces. By blending textiles' softness and flexibility with actuators' morphing capabilities, these interfaces offer a novel approach to designing interactive systems that can seamlessly integrate into our daily lives. However, creating complex fabric interfaces often requires new processes that are significantly different and incompatible with the standard approaches used to knit and weave fabrics. For example, many approaches to creating interactive fabrics require either: embedded hard components that diminish the affordances of cloth [5], complex digital design tools for implementation [14, 27], or require unintuitive manipulations of fabric [12, 20, 30, 35]. While these methods can produce unique fabric interfaces, they are estranged from traditional textile fabrication and machinery. Instead, we propose that creating a fiber that could be purchased as a raw material and is compatible with unmodified fabric machinery affords users the benefits of well-developed textile workflows while minimizing the approach-specific know-how and equipment.

To achieve this goal and facilitate the future of textile shape displays, we introduce FibeRobo: a morphing liquid crystal elastomer (LCE) fiber, and its fabrication approach to generate continuous lengths of such fibers with a desktop fiber drawing machine. The fiber exhibits a self-reversing contraction in response to thermal stimuli. We described two resin compositions that respond to different temperature ranges i) from 51°C to 86°C and ii) from 26°C to 66°C. The latter of which is responsive to body temperature. Our fabrication setup allows rapid production of continuous ultra-long (>100m) spools of FibeRobo that are compatible with textile fabrication processes such as embroidery, knitting, and weaving. All while being silent, inexpensive, and machine washable.

This paper presents a novel programmable actuating fiber, FibeRobo, compatible with many standard fabric manufacturing and prototyping techniques. We aim for FibeRobo to be easy for textile and interaction designers to adopt and create fabric interfaces. Briefly, this is done by 1) developing an automated, continuous, DIY, minimal-cost UV fiber spinning setup that will enable textile designers to create their supply of FibeRobo customized for their application, 2) adding sensing and actuation capabilities through the incorporation of heating elements or conductive coatings, 3) developing fabrication workflows for machine embroidery, weaving, and knitting FibeRobo with embedded heating elements, 4) creating the first body-temperature responsive liquid-crystal elastomer fiber for responsive wearables, and 5) developing illustrative demos to showcase the potential of FibeRobo for 4D textile displays.

2 RELATED WORKS

Textiles are a promising space for creating "intimate" [7] and tactile interfaces that can be worn on the body and integrated into everyday fabric objects such as clothing and furniture. Fabric affords flexibility and comfort where rigid electronic devices fall short [25]. Researchers have explored a variety of applications of e-textiles [3, 21, 27, 29, 38] and developed various techniques for creating interactive textiles. Across these techniques, three themes emerge. These are embedded hardware, textile engineering, and shape-changing and sensing materials. These approaches represent a tension between the practices of different stakeholders in e-textile design. Embedded hardware aligns e-textile design with the practices of interaction designers who already build rigid tangible interfaces. However, stiff and bulky components contradict fabric's soft and wearable affordances [7]. Engineering interaction between the textile and fibers can retain these affordances but introduces new challenges as novel materials are often incompatible with textile manufacturing techniques and design practices [41].

2.1 Embedding Hardware Into Textiles

The most common approach to creating textile interfaces is to embed hardware that actuates and senses the fabric. In a sense, these interfaces use textiles as a membrane for standard interactive components such as rigid buttons, slider knobs, LEDs, and microcontrollers. This approach can make designing textile interfaces widely accessible to interaction designers accustomed to working with electronics and has been widely adopted (e.g., LilyPad [5]). To align textile design practices with the practices of interaction and hardware designers, researchers have explored manufacturing techniques that integrate hardware directly into textiles. Hudson and Peng et al. embed rigid stiffeners into 3D printed fabric objects [26], and Rivera et al. developed a method for 3D printing rigid components onto textiles [30]. Albaugh et al. developed a machine knitting method for embedding tendons into a knitted fabric which a motor actuates [3]. Embedding artificial muscles into engineered fabrics can produce complex haptic interfaces. Kim et al. integrate these actuators into a knit sleeve that can locomote along the arm [16].

2.2 Engineering Textiles

Stretching beyond the limits of integrated hardware requires interactive properties (e.g., actuation, sensing) to be engineered into the textile. For example, Albaugh et al. created entirely knitted actuators by engineering spacer fabrics [4], and Luo et al. developed knitted capacitive sensors [19]. Multiple researchers have explored techniques for creating 3D-printed textiles using conventional FDM methods [8, 10, 35].

2.3 Morphing Fibers

Beyond engineering the textile and embedding hardware, researchers have taken a material science approach to create morphing fibers. Fabrics built with these fibers result in programmable fabric interfaces. For example, Kilic-Afsar et al. offer a robust actuating

Table 1: Comparison of fiber actuators in HCI literature. We report exact values when possible and appropriate. Green coloring highlights the particular strength of a given approach.

sProject	Actuator	Actuation Stimuli	Contraction	Actuation Speed	Hysteresis	Textile compatibility	Self-reversing
OmniFiber [1]	Mckibben	Pneumatic (requires loud pump/solenoid)	~32%	Fast (<1 sec)	Low	Machine knitting, weaving, hand sewing	Yes
ModiFiber [11]	Coated TCP muscles	Thermal (~60°C, silent)	~5%	Slow (~5 min)	Low	Hand sewing, weaving	Yes
KnitDermis [15]	SMA Springs	Thermal (~45°C, silent)	~50%	Fast (~1 sec)	High	Hand sewing/threading	No
FibeRobo	LCE	Thermal (~40-60°C, silent)	~40%	Fast (~8 sec)	Low	Machine knitting, embroidery, weaving, sewing	Yes

pneumatic fiber with high-frequency displacements and the ability to be knit and sewn [1]. However, it requires a bulky and noisy pump to actuate. Kim et al.'s *KnitDermis* [15] integrates shape-memory alloys into knitted structures to create textile shape displays. This work showcases the exciting potential for actuation-integrated fabrics for on-body wearable haptic effects such as twisting, compression, and pinching. However, the material requires manual intervention to reset the actuated fabric. Forman et al. develop a self-reversing alternative using silicone-coated twisted-then-coiled polymer muscles made from sewing thread [11]; however, producing such fiber is labor intensive, requires high temperature, has limited actuation (4%), and takes ~5 minutes to actuate. Actuation temperatures above body temperature can also present safety concerns for garments and other on-body applications [1, 11, 15]. In this regard, liquid crystal elastomer fibers bring great potential with their response time of ~1 second, a quick recovery time of up to a few seconds, and a tunable transition temperature below the body temperature [18, 31–33].

Existing implementations of self-actuating fibers have limitations in contraction length, speed, reversibility, and seamless integration into soft textile structures. Table 1 shows the properties designers must trade off to utilize a variety of morphing fibers. These properties are actuation stimuli, large contractions, low hysteresis (i.e., it can be actuated many times without wearing out), compatibility with textile tools, and the ability to self-reverse actuation.

Liquid crystal elastomers have emerged as a promising candidate for artificial muscle fibers. These solid elastic materials incorporate liquid crystal molecules that undergo a temperature-driven phase change from an ordered (isotropic) to a disordered (anisotropic) phase [32, 33]. In practice, these materials will change properties in response to temperature changes. For example, a material will shrink at one temperature and expand at a lower temperature. By controlling stimulus to the material (e.g., heating a fabric), we can program how the material behaves. LCEs are an attractive alternative to shape-memory alloys, which require extensive training for two-way actuation, have high hysteresis, and must be coiled to enable actuation above 5% [15]. In contrast, LCEs are self-reversing, hysteresis-free, and have large displacements of 40% without coiling [18]. Despite these advantages, LCE has been underutilized as programmable matter because, until recently, the actuation speeds were on the order of minutes, and transition temperatures were not skin-safe (60-150 °C). Two innovations in LCE synthesis and fabrication methods have addressed these barriers. Saed et al. reduced the transition temperature to 45°C, making it safe for actuation by body temperature [32]. Second, Lin et al. developed a streamlined technique to fabricate continuous LCE fibers [18].

Despite these advances, many challenges remain in integrating the interactive properties of LCE into textiles. First, the setup described by Lin et al. [18] produces fiber that fuses, making large spools impossible to produce. Second, LCEs fibers that actuate at skin-safe temperatures do not exist, and textiles using existing LCE fibers require high actuation temperatures of 60°C. Third, there has been little investigation into knitting, weaving, and embroidering these fibers to make higher-level morphing textile structures and interfaces with I/O integration. Silva et al. have preliminarily investigated morphing fibers into primitive woven structures, including twill and plain weaves; however, higher-level behaviors such as pleating and heating element integration for digital control are not explored [34].

3 GUIDING PRINCIPLES

The authors of this work include materials scientists, interaction designers, professional craftspeople, craft researchers, and researchers closely integrated into craft communities. These perspectives were used to derive three idealized guiding principles that enable a novel textile material to produce unique and novel e-textile designs and morphing fabric interfaces. In sections 8 and 9, we discuss the way and extent to which each criterion is fulfilled.

3.1 Integrated Interactivity

To function as an interface, the material and system powering it must be 'interactive.' The actuation should be quick, noticeable, and self-reversing. The material must be skin safe to be a tangible and wearable interface. Electrical control of the actuation (i.e., through resistive heating) is needed to connect the physical form with digital

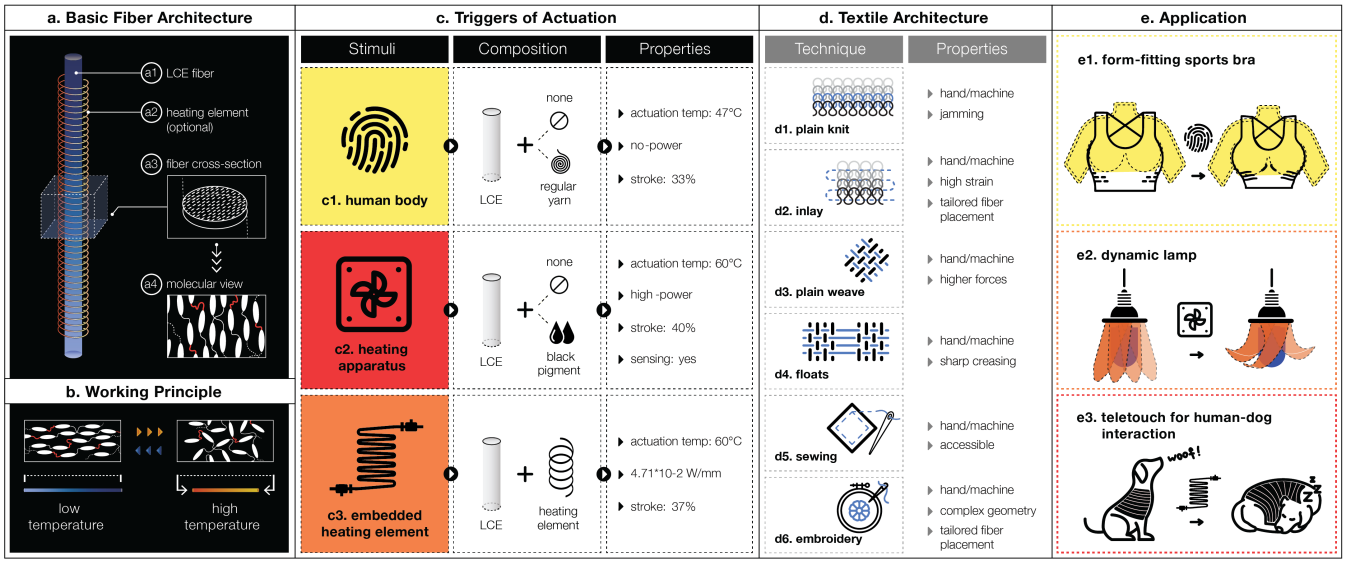

Figure 2: Pipeline from actuating fibers to 4D fabrics. From left to right 1) FibeRobo being produced in a custom UV drawing machine, 2) 750m of fiber produced in a day, 3) machine knitting with FibeRobo, 4) weaving with FibeRobo, 5) a telepresence canine compression jacket.

computation and sensing. Such integration should be done seamlessly without compromising the soft and flexible affordances of fabric.

3.2 Process Compatibility

To access the extensive capabilities of well-developed textile fabrication approaches, FibeRobo needs to have the affordances of standard fibers. It should be able to be manufactured to abundant lengths allowing designers to cut, tear, knot, and scrap the fiber without a second thought. The fiber must also be compatible with many different textile manufacturing techniques. For example, like conventional fibers, LCE fibers must have a consistent thickness so that they do not jam machinery; and be thin but with sufficient mechanical strength so that it does not break during use. While the fiber plays a lead role in the finished product, it should vanish into the chorus of materials during fabrication. The ultimate goal of process compatibility is craft-person compatibility – meaning that craftspeople can create interactive fabrics without substantially altering their practices. Since this requires external validation outside the scope of this work, we focus on producing a fiber that works on the most basic levels with the common tools and techniques employed by textile designers.

3.3 Modifiable Materiality

Textiles have applications spanning space suits, prosthetic liners, and couture. Each domain has its own design specifications, fiber requirements, and fabrication approaches which vary considerably. In the same way that SMA can be purchased in a range of diameters and actuation temperatures, FibeRobo should work across various actuation temperatures, allow different diameters and colors, and afford different sensing capabilities. For example, we should be able to program the actuation of the yarn to respond to specific temperatures at specific speeds. In addition, the fiber should be adaptable to allow the actuation stimuli (e.g., light, heat, electricity) to change.

4 FIBEROBO MATERIAL

In this work, we use advances [18, 32] in liquid crystal elastomer fabrication to create a morphing fiber that meets our guiding principles and can create interactive textiles. At lower temperatures (e.g., room temperature), the crystal molecules in an LCE are aligned to form a stretched-out material. As the temperature increases, these molecules fall out of alignment and cause the material to contract. To create FibeRobo, we synthesize a liquid resin containing LCE molecules. This resin can be extruded into even fiber strands and cured into a solid fiber using UV light. The resulting solid fibers are flexible and elastic with heat-responsive actuation.

5 FABRICATING FIBEROBO

To follow the principle of process compatibility, FibeRobo must be manufactured with a quick continuous process to create hundreds of meters of fiber. At these lengths, the fiber is non-precious and can be shared and worked with like any other fiber without fear of wasting hours of lab work. Additionally, long fiber lengths are necessary for uninterrupted knitting, weaving, and embroidery of larger samples and applications. We have developed a low-cost continuous LCE fiber drawing machine to create FibeRobo at these lengths and with material properties compatible with various textile production methods.

With this machine, FibeRobo is relatively inexpensive to produce. At our current fabrication scale, LCE with a diameter of .5 mm has a material cost of ¢20/meter. For context, this is 30-60

times less expensive than SMA of the same diameter, which costs $6.25-$12.50/meter [44]. Our labor cost is nominal since a single team member can easily synthesize and draw 750 meters of LCE fiber in a single workday. To enable the adoption of FibeRobo, the process and materials for replicating the machine are described in the Supplementary Materials. We provide these instructions in alignment with modifiable materiality to aid makers in producing fibers with properties explicitly tuned to their applications. While the resin synthesis requires a fume hood, spinning and working with the resulting fiber can happen anywhere. Still, the need for a ventilated hood and machine-building experience limits the accessibility of reproduction; however, we only intend for this to be a temporary solution to allow external replication and experimentation. In *Reconfigurable Elastic Metamaterials* Yang et al. [40] pursue an alternate strategy to making their metamaterials accessible by designing them to be a commercial stock material. Similarly, since FibeRobo can be cheaply and continuously produced, we envision it being a commercial product that people can buy in varieties and directly use on their unmodified textile machinery.

To make the fiber, we adopt Lin et al.'s method for continuously spinning LCE fibers by extruding LCE inks through a 3D-printed nozzle [18]. Instead of depositing the inks onto a surface, the filaments are pulled onto a rotating coil and cured midair via two UV LEDs. We address two critical limitations of this spinning process that limit the process compatibility of the resulting fiber. First, limited UV exposure and the absence of a coating process result in fibers that fuse if layered, making large spools impossible. We address this by using UV-led strips to increase UV exposure along the length reducing the tendency to fuse. We dip the fiber in mineral oil mid-cure to create a barrier between fibers. Second, the fibers produced with the prior approach coiled, making them incompatible with common textile equipment such as embroidery and knitting machines. The coiling is due to the fibers only being cured on one side, creating a quasi-bilayer structure that curls. We addressed this by including Waveform Lighting 365 nm UV strips on both sides of the fiber, balancing the curing and allowing faster spinning speeds. We also increase the photoinitiator concentration to 2 wt% to increase the crosslinking speed. Third, the prior approach requires an expensive ($1,000) print head (Hyrel KR215[1]) that requires ~$200 15ml stainless steel cartridges making bulk ink preparation costly. Instead, we developed a low-cost syringe pump using 3D-printed and inexpensive parts. Our complete syringe pump (including motor drivers, heating elements, and thermo-coupling) comes to ~$250. Additionally, we can customize the syringe holder for 5, 10, 20, or 30 ml high-pressure polyacrylamide syringe cartridges at ~$4/piece, allowing ample batch preparation. Beyond that, we developed a UV-blocking acrylic enclosure that allows safe observation of fiber spinning and reduces wind.

In the following subsections, we detail the process of fabricating FibeRobo. We start with how we produce the LCE resins. Then we describe the construction and use of our spinning machine. Third, we describe optional post-processing steps to turn FibeRobo into a sensing and actuating fiber. Finally, we detail key safety considerations.

[1]https://www.hyrel3d.com/portfolio/kra-15/

5.1 Resin Synthesis

This section describes the process for creating the precursor resins for fiber synthesis. Along the principle of modifiable materiality, we describe two compositions with two different actuation temperatures (65°C and 47°C). The *Appendix* contains advice for successful synthesis, the full name and qualitative description of each raw material, the purpose of each component, and their purchase origin.

5.1.1 High-temperature High Contraction Fiber Resin Preparation. 15 g of RM82 and .105 g of BHT are added to a glass vial and placed in a 110°C toaster oven until completely melted. 4.5 mL of EDDET and 800 μL of TATATO are added to the vial and mixed. The vial is returned to the oven until completely clear. Next, 0.42 g of I-651 and 100 μL of DPA are added to the vial and vigorously mixed. The solution is centrifuged at 3,000 RPM for 3 minutes to remove air bubbles. In the Supplementary Materials, we also describe an alternate centrifuge-free procedure. The rubber seal is then maneuvered into a syringe, and a 3D-printed high-strength plunger is added. The syringe can now be stored in a cool dark place for up to one week before use. However, if more than a day has passed, the resin should be heated to 80°C to reset the material.

5.1.2 Low-temperature Low Contraction Fiber Resin Preparation. By combining RM82 with RM257, the transition temperature is lowered from 65°C to 47°C; however, the actuation displacement is reduced from ~35% to ~31% (see Table 2). The process for resin synthesis is similar to that of high-temperature resin, with some differences. First, 15 g of RM82, 5 g of RM257, and .62 g of BHT are added to one vial and melted at 80°C. At the same time, 7.5 mL of GDMP is preheated in a separate vial at 80 °C. In rapid succession, the two vials are mixed, and .47 g of I-651 and 1.7 mL of TATATO are added and mixed vigorously. Finally, .47 mL of TEA is added, combined, and transferred to a syringe before centrifuge degassing.

5.2 Continuous Spinning

Our machine, shown in Figure 3, includes 1) a temperature-controlled syringe pump for extruding high-viscosity fluids, 2) a drawing spool to align and thin the fibers, 3) UV light channels to cross-link and cure the fiber, 4) a dip coat stage to coat the LCE fiber in generic mineral oil to ensure easy unspooling, and 5) a UV blocking enclosure to ensure safe viewing of the drawing process.

In this machine, fibers are formed in a four-step process. First, the resin is preheated in the syringe pump to ~34°C to lower its viscosity and facilitate extrusion. In Step 1, the resin is extruded out of the syringe. In Step 2, the fiber is cured by UV light. The fiber is then grabbed with tweezers, easily stretched around the pulley spool through the second UV light channel (Step 3), and collected in Step 4 onto the final spool.

During drawing, four main parameters affect the properties of the resulting fiber. These are 1) extrusion speed, 2) pulley speed, 3) uptake spool speed, and 4) UV light intensity. When properly coordinated, these parameters result in stable fiber spinning for the entirety of the loaded syringe. For a given extrusion speed, a forgiving range of uptake and pulley speeds will work and tend to vary slightly by batch. An in-depth analysis of the general process is given by [18].

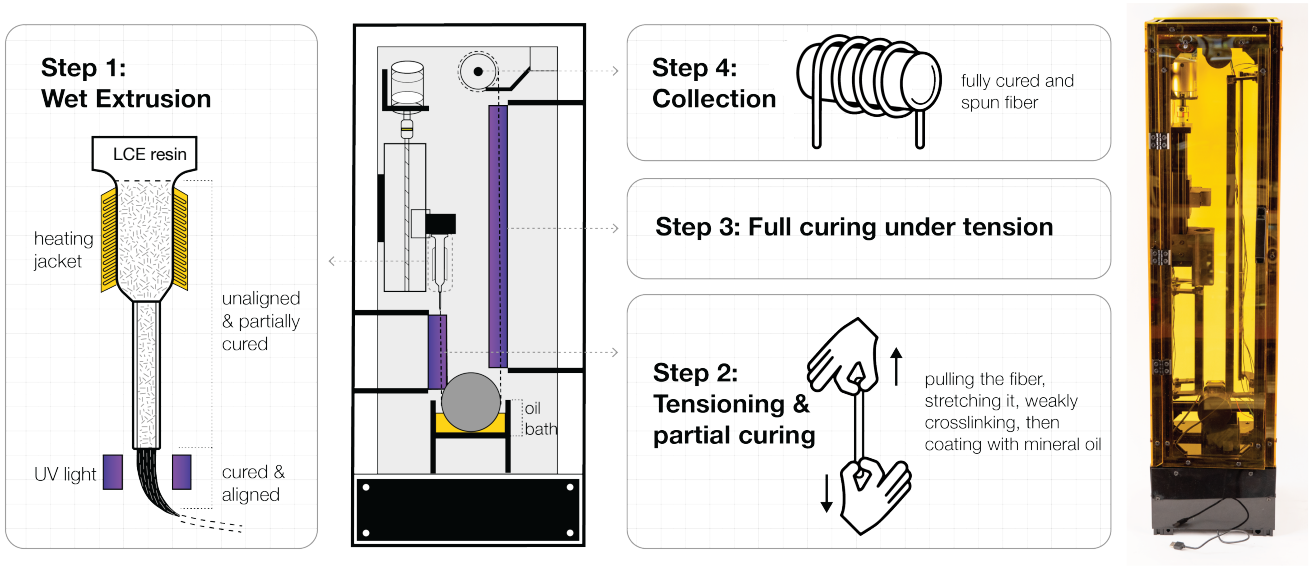

Figure 3: Overview of the fiber fabrication process. First, a viscous resin is extruded, stretched, and cured with UV light. Then the fiber is dipped in oil, and the UV curing is completed as the fiber ascends to the final collection spool.

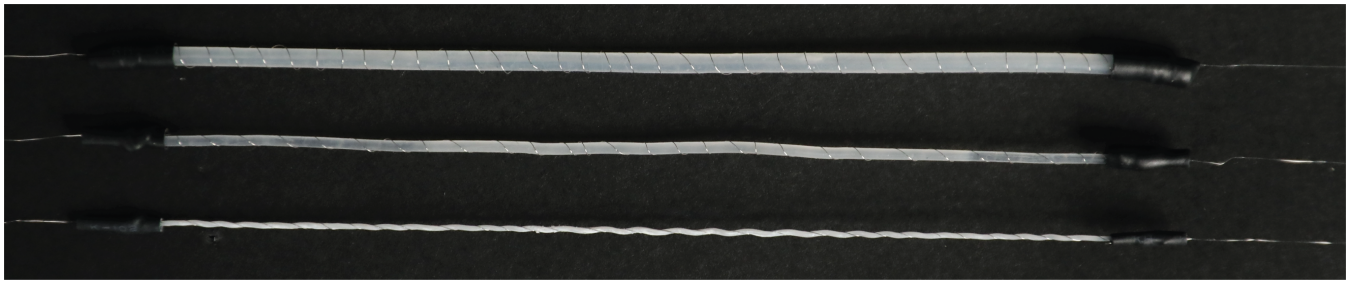

Figure 4: FibeRobo with different diameters of 0.5 mm, 1 mm, and 2.0 mm (bottom to top) plied with conductive wire.

Generally, the fiber diameter decreases as the uptake and pulley speed increase; however, the stroke of the fiber will remain the same as the liquid crystal is already fully aligned from the extrusion. As previously noted, another important parameter is the UV light intensity of the first curing channel. If the UV light is too dim, the fiber will separate during the drawing process. If the UV light is too bright, clumps can form and clog the nozzle, resulting in uneven, bumpy fibers. However, once stable parameters are found, the entire syringe can be formed into the fiber without stopping or breaking. Our device includes a PWM dimmer that allows us to tune this brightness on a case-by-case basis. Details on our specific spinning parameters are included in the Supplementary Materials. The fiber is then unspooled and dusted with talc powder to facilitate low-friction movement of the thread when driven through yarn carriers and tensioning mechanisms in various textile processes such as embroidery and knitting. Once formed into a fabric, the powder can be washed away with warm soapy water.

5.3 Post-Processing: Twining, Braiding, and Dyeing

We can modify the materiality of the fiber by adding sensing and resistive heating capabilities by post-processing the basic morphing fiber to incorporate conductive wires and coatings. Following the principle of integrated interactivity, the solution proposed should be elegant and robust without compromising the soft and flexible nature of the fiber.

5.3.1 Twining and Braiding with Heating Element. In some cases, users may desire a single fiber with an integrated heating and/or sensing element to use as a basic tendon actuator. This can be achieved by combining FibeRobo with a conductive thread to create a composite thread with resistive heating and capacitive sensing elements, as shown in Figure 4. Plying is the traditional technique for combining two threads by twisting them; however, this technique is unsuitable for FibeRobo as the twisting results in torsional actuation making textile actuation unpredictable. The heating element must be wrapped around the LCE fiber for linear actuation. Doing so is quickly achieved by hanging the LCE fiber from a drill

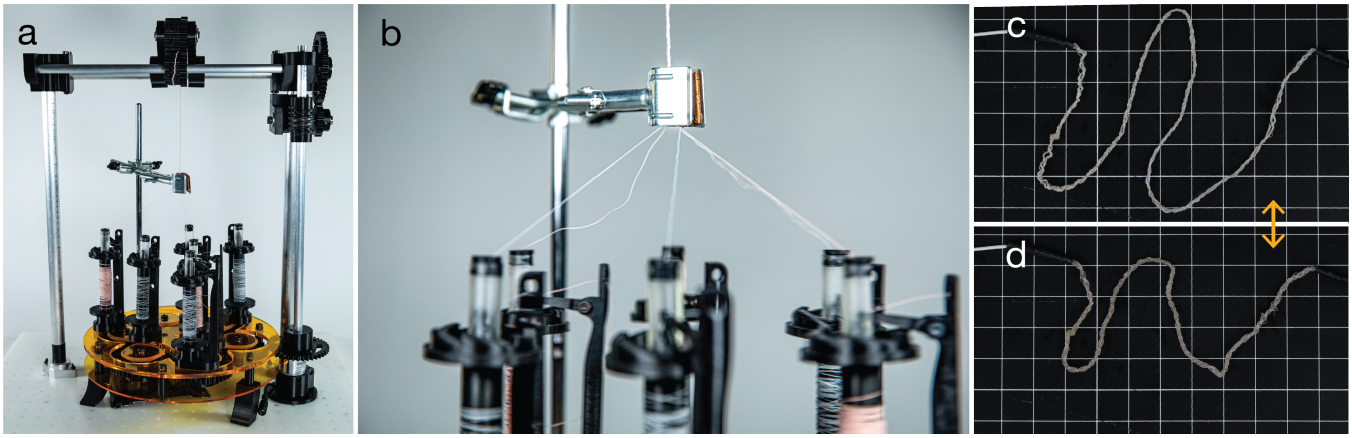

Figure 5: (a) a DIY Maypole braiding machine prepped to produce a braided actuator. (b) a close-up of the braiding process that combines 4 LCE fibers with two litz wires. (c) A 34.5 cm FibeRobo/lite wire braid without electrical power (d) the same braid 8 seconds later, now 21.6 cm, after being powered with 2.5A and 8.5V. Once we remove the power, the fiber returns to its original length after 30 seconds.

with a 5g weight. The drill is then spun as the hand guides the winding of the conductive thread around the fiber.

While the plying process is useful for the early-stage production of short fibers, it is too tedious for longer lengths. As a solution, we recreated an open-source DIY Maypole Braiding machine [37] shown in Figure 5a-b to quickly make long, stable, non-twisting, multi-ply fibers with embedded heating and sensing wires. While the braiding introduces some twist, we can easily create a non-twisting braid by keeping an equal number of FibeRobo strands on each side of the braid, forming a torque-balanced structure. This specific machine allows up to 6 fibers to be combined, allowing a variety of combinations such as including two wires; one could be a heating element and the other a capacitive sensor. For the heating elements, we use litz wires (10/44, Mike's Electronic Hardware) which are strands of enameled copper shielded with a textile braiding. The thin form factor and textile shielding afford the appearance and feel of a regular thread. They have a copper core, so their resistance is lower than most conductive threads. This low resistance is more conducive to faster heating and larger scales. We use a silk-coated litz wire instead of synthetic conductive threads as it does not shrink or melt when heated. We also found hand braids to be perfectly functional, albeit labor-intensive, for prototyping. Figure 5 shows the braid in the unactuated (5c) and actuated (5d) states. With 2.5A and 8.5V, the braid contracts 37% in 8 seconds and reverses back to its original length in 30 seconds. From the power parameters, we can derive the minimum normalized power per unit length of the braid to be 4.71*10-2 W/mm.

These hybrid fibers are not recommended for knitting, weaving, and embroidery as they may cause pile-ups and unpredictable fabric actuation. For these three processes, we suggest that the conductive fiber should be integrated separately. We describe and verify the workflow for each in section 7.

5.3.2 Conductive Carbon Black Dyeing. As a continuation of integrated actuation, we developed a process to add a conductive coating onto the fiber's surface to enable capacitive and stretch sensing. We adopted an absorption approach for creating electromechanical cell culture surfaces [2]. We produced conductive LCE fibers and fabrics by soaking samples in a 7 wt% Carbon Black (CB) and toluene solution. The samples were immersed in the dye for 6 hours, then dried in an 80 °C oven for 1 hour.

5.4 Safety

Again in the spirit of integrated interaction, FibeRobo is intended to be used by researchers and textile designers for various applications, including on-body wearables. As such, the safety of the material was a priority. We selected compositions with confirmed biocompatibility and a solvent-free synthesis process that minimizes the use of hazardous materials and waste. In short, the final fiber is completely safe, but some precautions are needed for the synthesis.

First, the resin synthesis and carbon black dyeing should be performed in a fume hood with gloves, a coat, and goggles. However, once the resin is prepared, it is non-hazardous, as several works have studied the biocompatibility of LCEs with a composition nearly identical to FibeRobo. Specifically, Yakacki et al. found no cytotoxicity for the fiber resin and the fully cured LCE [39]. Further studies have supported this claim saying, "These findings are strong evidence towards verifying LCEs as a safe and stable material for use in physiological conditions and fulfilling applications as a biomaterial" [33]. Once cured and solidified, the fibers can be handled and worked with normally. As a note, the fully cured fiber has no discernible smell providing immediate, albeit qualitative, evidence of complete crosslinking.

A mild hazard [45] is that UV eye protection should be worn when observing the 365 nm UV lights used to cure the fiber. As a result, we use UV-protective glasses when the door is open. We also built an acrylic enclosure with an inexpensive yellow film that blocks 99% of UV light allowing close fiber spinning observation without glasses.

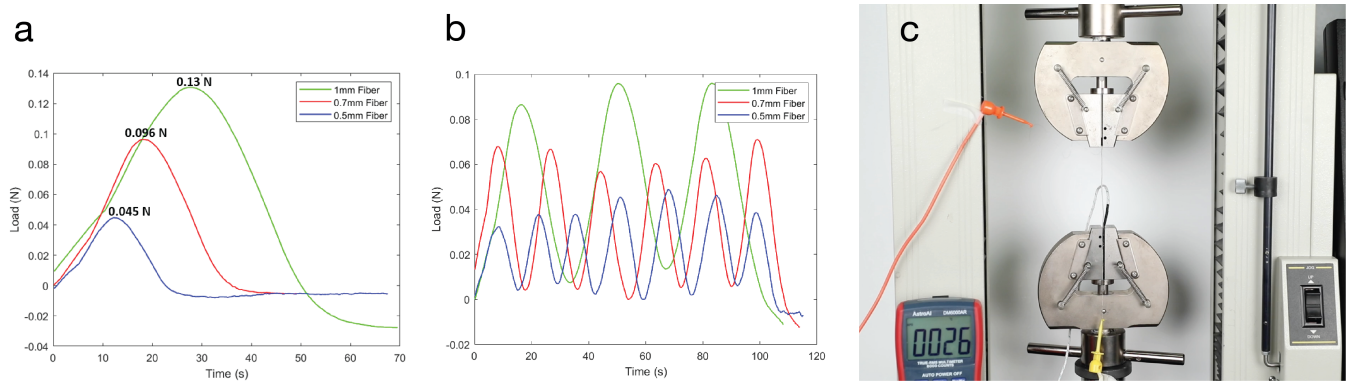

Figure 6: FibeRobo mechanical characterization; (a) peak loads achieved upon heating (followed by cooling) FibeRobo fibers of different diameters (1mm, 0.7mm, and 0.5mm); (b) thermal cycling response of FibeRobo fibers; (c) test setup used to measure loads on the Instron Universal Tester, with temperature measured using a multimeter, and fibers heated with conductive thread.

Table 2: Comparison of LCE fibers at different actuated temperatures

Resin Type	Lit. Ref.	Total Stroke(reported vs. measured)	T_{ni} On-set(reported vs. measured) °C	T_{ni} Off-set(reported vs. measured) °C
#1 (high temp)	[18]	35% : 38%	51±1 : 40±5	86±1 : 80±5
#2 (body-temp)	[18, 32]	31% : 33%	26±1 : 30±5	66±2 : 60±5

6 FIBER CHARACTERIZATION

This section demonstrates the actuated stroke generated in FibeRobo, the mechanical forces generated, and the response to thermal cycling. As discussed earlier, we can tune the actuation temperature of the fiber through different resin compositions. Here we characterize these fibers to aid in material selection and to support modifiable materiality.

6.1 Temperature vs. Actuation

We intentionally selected existing LCE compositions that prior works have thoroughly characterized. Still, we devised a frugal test for researchers to quickly validate and measure the Tni onset (actuation start temperature), Tni offset (actuation end temperature), and contraction ratio. The validation begins with 8cm fiber samples immersed in a 100°C water bath with a thermistor. The water is allowed to cool, with length measurements recorded at 10°C intervals. This process enables the Tni offset, Tni onset, and contraction ratio to be measured. Table 2 shows the resulting values compared with the referenced literature.

While the body-temperature composition only reaches full actuation at 66±2°C, the majority of the actuation occurs at the Tni midpoint of 47±2°C which is below pain thresholds [32]. In our experience, heating the body temperature fiber on the skin feels mildly warm.

6.2 Diameter vs. Load and Thermocycling Speed

In this section, we measure the effect of varying fiber diameters (0.5mm, 0.7mm, and 1mm) on the speed and force of actuating fiber. Fibers wrapped in a thin wire, similar to those in Figure 4, were loaded into an Instron Universal Tester under negligible tension. Since the fiber is statically held during actuation, the helical coil wrapping does not add significant loads. The fibers were resistively heated with 0.2A (Voltage was ~15V, but this depended on the exact length/resistivity of the sample). Figure 6a shows the load vs. temperature curves for a single slow cycle. As expected, the force scales with the diameter of the fiber, with the thickest fiber producing the highest loads.

The fibers were repeatedly cycled between their maximum and minimum loads with 0.2 A of current (Figure 6b). Although the thinnest fibers produce less force (0.045 N) than the thickest fibers (0.13 N), they can cycle much faster (~6.66 cHz) than the thickest sample (~2.86 cHz). The faster cycling of the thinner fiber is owed to a greater surface area to volume ratio, meaning the fibers can absorb and dissipate heat more rapidly. Since the load scales linearly with the number of fibers [18, 31], one could likely achieve rapid high-force actuation by combining many tiny threads into a woven fabric. Note that the current used for heating was conservatively low to allow clear comparison and temperature measurements, and faster actuation is likely possible with a higher current.

6.3 Strain vs. Resistivity

In this section, we characterize the piezoresistive behavior of a carbon black coated FibeRobo for a single fiber, a woven fabric, and a knit fabric. As described earlier, FibeRobo can be coated in carbon black, allowing the fiber to act as a resistive stretch sensor. As the fiber stretches, the carbon black coating becomes thinner and disrupts, thereby increasing the resistivity of the thread. Figure 7a shows the difference in surface texture in relaxed (top) and stretched (bottom) states. To characterize the change in resistance due to stretching, we loaded a 5cm long 750 μm carbon black coated

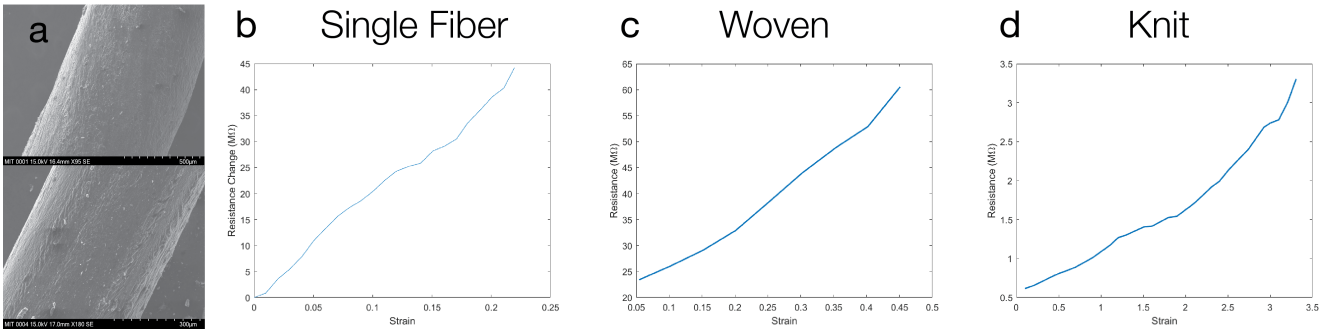

Figure 7: Carbon black coating for resistive sensing: a) top: an unstretched 857-micron fiber coated in carbon black, bottom: the same thread (now 488 microns in the stretched state). b) resistance change due to fiber stretching. c) resistance vs. strain for a plain woven sample with embedded FibeRobo. d) resistance vs. strain for a 2cmx5cm knitted band

fiber into an Instron Universal Tester. The resistance is 11.72 MΩ at rest and 55.9 MΩ at 22% elongation. As shown in Figure 7b, the change in resistance due to strain is roughly linear. While no resistance could be measured after 22% elongation, the conductivity is quickly restored once the fiber is released. When actuated, the resistance is 2.03 MΩ.

For the woven characterization shown in Figure 7c, we prepared a 10x10 cm plain weave, with three rows in the middle being a single conductive Fiberobo with a 1mm diameter. The Instron stretched the sample along the elastic weft to generate a strain vs. resistivity plot. It exhibited a linear increase starting at 20.95 M Ohm and ended at 60.55 MΩ at 45% strain before reversibly losing conductivity. The durability of the coating was assessed by measuring the resistivity of the fiber before and after weaving. These measurements revealed an increase from .21 MΩ/cm to 0.54 MΩ/cm, indicating some degradation, albeit still functional.

For the knit characterization shown in Figure 7d, we prepared a 2x5cm knit conductive strip and measured the strain vs. resistivity on the Instron. The behavior was also roughly linear: it started at 0.603 MΩ and ended at 3.304 MΩ at 350% strain, after which the knit ripped. The fiber's ability to maintain conductivity despite large strains is owed to the inherent stretchability of knits and the lowered resistances are due to the inter-knitting of the conductive fiber, which creates multiple conductive pathways. The durability of the coating was assessed by knitting another 2x5cm, then unraveling it and comparing resistivity. The 1mm coated fiber had an initial resistance of .23 MΩ/cm, whereas the resistance increased to .609 MΩ after knitting and unraveling, indicating some non-critical degradation.

7 FABRICATING WITH FIBEROBO

Once we produce the fiber, we can employ techniques that traditionally use non-reactive fibers. A key benefit of FibeRobo is its compatibility with standard textile manufacturing techniques and machines. This feature speaks to process compatibility as we can integrate shape-changing properties into various textiles and garments without modifying textile designers' equipment.

The following subsections present demonstrative interactive textile designs made with FibeRobo. We organize these demonstrations based on the textile manufacturing process we used to create the design and characterize the critical properties of FibeRobo that made it compatible with these crafting practices. We also outline the best practices and parameters we found essential for prototyping.

7.1 Embroidery Compatibility

Embroidery involves using hand- or machine-based methodologies to sew patterns with thread onto a material. A person or machine uses different stitches and threads to create images and unique textures on top of a fabric. Embroidery with FibeRobo allows us to augment existing textiles with morphing motifs. Through careful design of the stitch density and patterns, we can construct different morphing primitives using both hand and machine embroidery techniques.

7.1.1 Hand Embroidery Application - FibeRoBra: Adaptive Sports Bra. In Figure 8, we developed a morphing bra to illustrate FibeRobo's responsiveness to body temperature and sewing compatibility. In the rest state, the bra provides relaxed support with some contraction. Once the user begins exercising and their body temperature increases, the fibers contract around the breasts providing additional support; as the user cools down, the bra will become loose again. This application also demonstrates how the modifiable materiality of the fiber enables integrated interactivity. By designing the actuation temperature of the resin to be responsive to body temperature, we enable passive sensing and actuation on the body with no additional hardware or wiring. The resulting bra is interactive but entirely made of fabric.

7.1.2 Machine Embroidery Application - FibeRoGlow: Dynamic Lamp. In this application, we demonstrate FibeRobo's responsiveness to ambient heat sources and compatibility with embroidery machines. The self-reversing actuation shown in Figure 9 takes ~5 minutes in each direction. While this actuation is relatively slow, this demo shows that FibeRobo does not require direct coupling with a heating element for controllable actuation. Light, or infrared heating, are two potential modes of remotely controlled actuation.

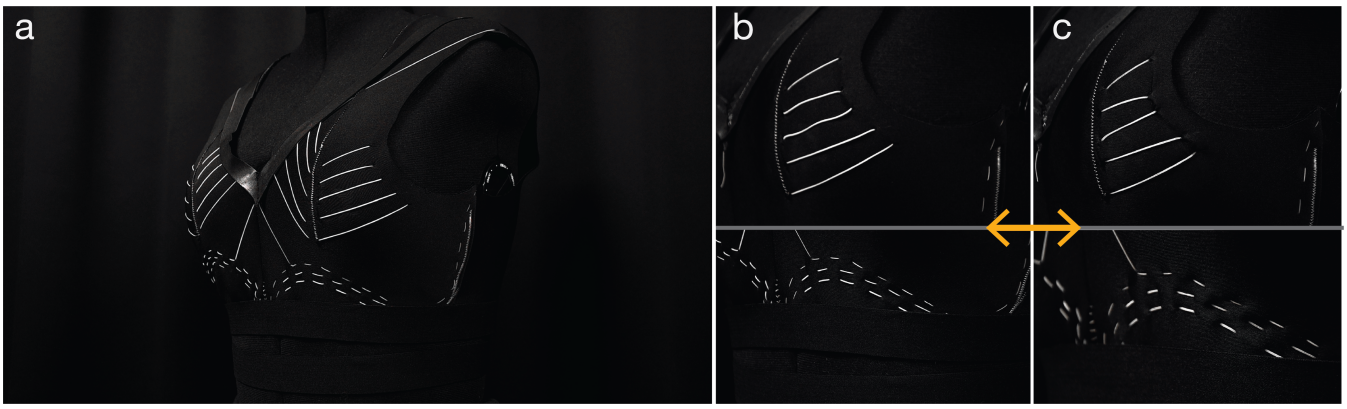

Figure 8: An adaptive support sports bra with hand-sewn continuous FibeRobo patterns. (a) sports bra prototype on a medium-sized mannequin, (b) a close-up image showing the unactuated state, and (c) the actuated state.

Figure 9: In this application, we demonstrate the aesthetic affordances of 'livingness' with a blooming lamp. When one turns on the light, the heat warms the fibers causing them to contract and lift the petals.

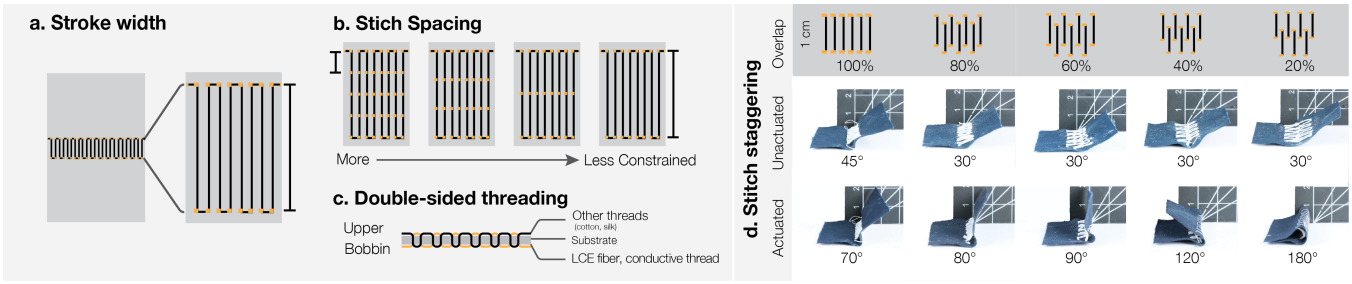

Figure 10: (a) Stroke width, (b) Stitch spacing, (c) Double-sided threading, and (d) Staggered stitches lead to different folding angles.

7.1.3 Embroidery Development: Stitch Density. For these demonstrations, we use embroidery tools employed widely by textile makers. We use a Brother SE500 machine and two open-source embroidery programs to explore stitch design: for detailed line work, we use PEmbroidery [42], and for organic geometries, we use Inkstitch. We also explored a variety of fabrics, including cotton, neoprene, organza, and dry oilskin. The sample in Figure 11 was done on dry oilskin fabric with a 200-micron thread diameter to modulate bobbin tension, and silk thread was paired with the FibeRobo to create a bilayer actuator.

Sample characterization involved iteratively varying stroke width, stitch spacing, and double-sided threading(Figure 10, a-c). Stroke width (Figure 10a): the larger the width, the larger the displacement of LCE fiber, thus more considerable deformation. Stitch spacing (Figure 10b): the larger the stitch spacing, the less the constraint between the substrates and threads, therefore, larger deformation. Double-sided threading (Figure 10c): LCE fiber is placed at the bobbin, while other threads are at the upper. Stitches staggered with the minor overlap led to sharper pleat actuation (Figure 10d).

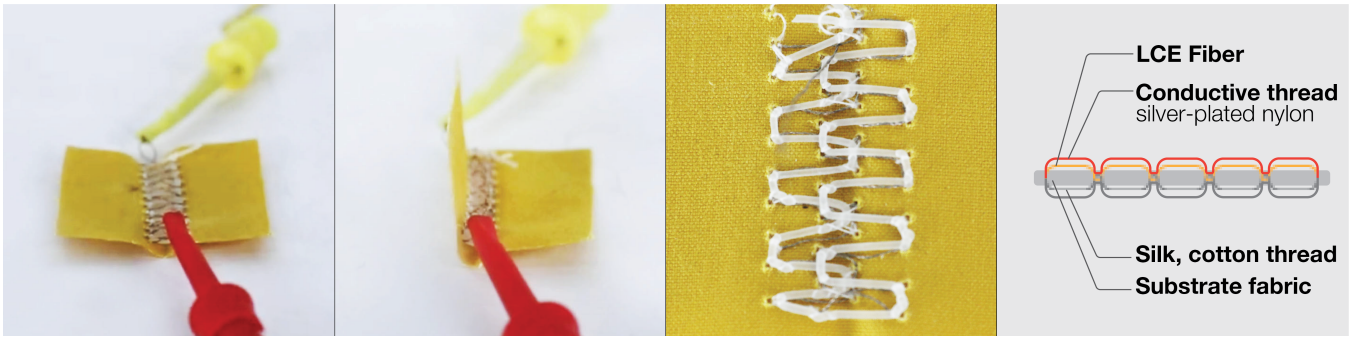

Figure 11: A pipeline integrating LCE fiber with heating elements through machine embroidery. (a) Unactuated state, (b) Actuated state through 0.1A and 5V power supply, (c) A close-up image of LCE fiber and conductive thread, (d) an illustration showing the fiber placements on the fabric substrate.

7.1.4 Embroidery Development: Integration of a Heating Element. In addition, we explored the machine embroidery integration of LCE fiber and conductive thread. (Figure 11). This implementation used LCE fibers and conductive thread as the bobbin thread because of the LCE elasticity and conductive thread stiffness. As a result, this is a two-step process where the LCE fiber is first loaded into the bobbin and embroidered with a Brother SE500 machine. We then repeat the embroidery with a conductive thread (silver-coated polyamide, AGSIS) bobbin. The conductive thread was used instead of litz wire as the litz wire tended to jam the machine. We used a cotton thread as the top thread for both.

7.2 Weaving

Weaving involves interlocking warp and weft components to create a fabric structure. Woven designs can transform into complex, multidimensional structures for soft goods, apparel, and interior applications by manipulating the placement of warp and weft threads. Researchers have previously used LCE fibers to create intelligent textiles by hand sewing them into woven fabrics [31]. However, they had to heat the woven material to 80°C to actuate, risking harm to human skin when worn directly on the body; this is similar to most other thermally triggered textiles requiring high actuation temperatures [11]. Our woven embodiments use a body-temperature fiber with a transition start temperature as low as 30°C. Additionally, in our approach, we also directly weave with the LCE fibers and take advantage of the woven structure's precise ability to determine actuation geometry.

7.2.1 Weaving Application: ShadeRobo. In this application, we demonstrate ShadeRobo (Figure 12) for silent shape-changing curtains. Without the presence of thermal stimuli, the curtains cover the window. The curtains rise once current runs through the fabric, revealing the window. In this demo, we do not want the fiber to be responsive to sunlight-induced heat, as we want the curtain to block the light. By applying the principle of modifiable materiality, we use the higher-temperature fiber for actuation and the litz wire for resistive heating. For this 5cmx5cm swatch, we use 4V and 2.5A to actuate the fabric. The fabric reaches full contraction in two minutes and reverses to its original form after one minute of cooling. While we can increase the actuation speed by including more litz wire, rapid actuation is unnecessary for this application. Instead, we prioritized minimizing the power demands by only integrating 8 rows of litz wire for actuation. Unlike other automated retractable curtains, the actuation of ShadeRobo is entirely silent.

7.2.2 Weaving Development: Floats. In Figure 13, we leverage woven fabrics with float structures to create sharp pleats upon actuation. A weaver creates floats by skipping one or more wefts over warp ends, creating two layers of connected fabric with different structural densities. Other ways to achieve similar effects may include pleating, sewing, and integrating complex weave structures. Our handwoven samples distinguish themselves from alternative techniques by the structural actuation involving no post-production manipulation. Our strategic placement of FibeRobo enables the transition from a two-dimensional to a three-dimensional form. Hence, we achieve the accordion form (Figure 13) through 5 mm long float structures on the woven sample's front and back.

Figure 13 also demonstrates how we tested different float lengths for woven structures; this investigation provided insight into how the actuation potential and the sharpness varies based on LCE float lengths. By creating floats of 0.5cm, 1.5cm, and 2.75cm as vertical and diagonal weft structures, we strategically placed floats on the front and back of larger woven samples to create multidimensional, origami-like folding designs. Weft floats were intentionally staggered based on warp threads to increase the sharpness of the pleating, which is the most visible in the samples with a float length of 0.5cm. This investigation highlights how the actuation potential and the crease sharpness of each of these LCE float lengths provide a framework for the future exploration of actuated, origami-inspired woven structures.

7.2.3 Weaving Development: Integration of Heating Element. We explored weaving LCE fibers with a silk-covered litz wire which acts as a non-elastic heating element (10/44, Mike's Electronic Hardware). We utilized these heating elements with 8cm by 8cm woven samples, each containing a float length of 1.5cm. As a result, we created a stable, reversibly actuated woven structure that we can digitally control through joule heating (Figure 14, a-d).

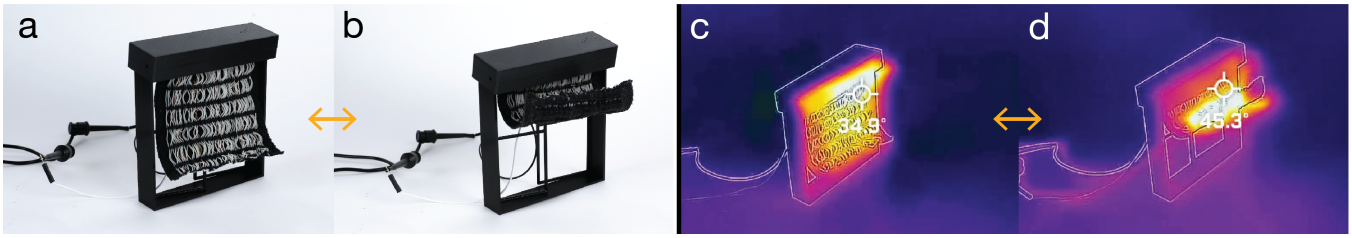

Figure 12: A demonstration of how heat actuation influences the form of window application through an 8x8cm woven sample with FibeRobo and silk-coated nichrome wire. (a) ShadeRobo with no heat; (b) ShadeRobo responds to a current of 4V and 2.5A that is run through a silk litz wire. (c) thermal imaging of the unpowered curtain; (d) thermal imaging of the powered curtain.

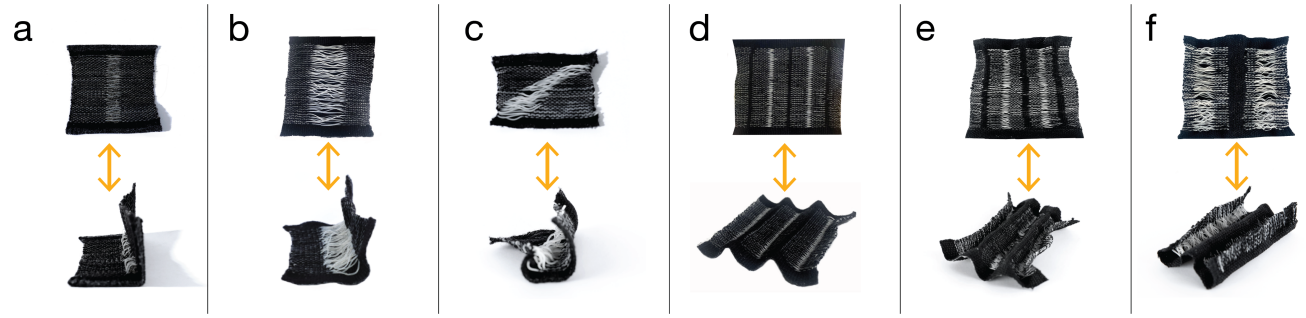

Figure 13: 8cm x 8cm woven samples with FibeRobo; (a) top: a woven piece with nano-plated silver conductive weft threads and a 1.5cm LCE float, bottom: the actuated state of the sample; (b) top: a woven sample with a 2.75cm LCE float, bottom: the actuated state; (c) top: a woven sample with a 1.5cm LCE diagonal float, bottom: the actuated state; (d) top: a woven sample with five 0.25 cm floats on alternating sides of the fabric, bottom: the actuated state; e) top: a woven sample with five 0.5 cm floats on alternating sides of the fabric, bottom: the actuated state; (f) top: a woven sample with five 1 cm floats on alternating side of the fabric, bottom: the actuated state.

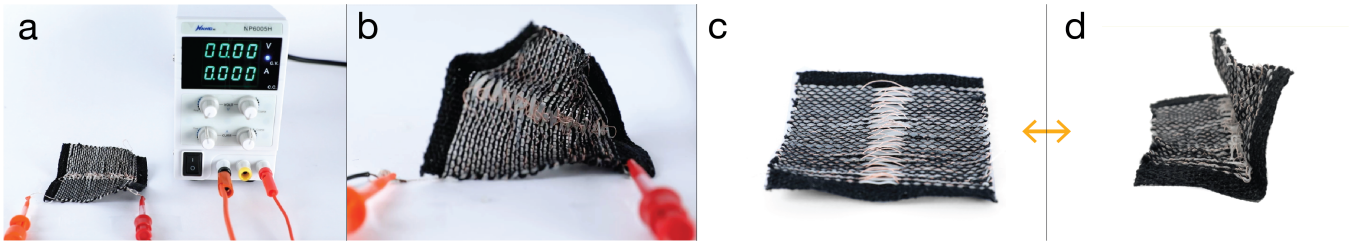

Figure 14: Demonstration of how heat actuation influences the form characterization of woven fabric samples using LCE fibers with float lengths of 1.5cm. (a) demonstration of heating set up; (b) fabric form response to 2.5 amps and 4 V; (c) closeup of the unactuated state; (d) closeup of the actuated state

7.3 Machine Knitting

In knitting, a continuous yarn is interlocked into a grid of loops to form a fabric. Knitted textiles are typically more breathable, making them an attractive textile architecture for abundant use cases, including but not limited to comfort wear, sportswear, and medical textiles [1].

7.3.1 FurbeRobo: Short-range Teletouch for Human-Dog Interaction. In this demo, we develop a knitted compression shirt that allows its owner to send their dog a calming hug from afar. During knitting, we embed the jacket with a heating element controlled by a microcontroller. The heat causes knitted FibeRobo to actuate and compress around the dog. Compression jackets are a conventional method for alleviating the separation anxiety experienced by a dog when its owner is away and has been shown by King et al. to significantly reduce markers of anxiety, including increased heart rate [17]. Unlike other compression garments (e.g., [6, 9, 23, 36]) that use bulky inflatable vests, noisy pumps, or uncomfortably high actuation temperatures that require insulation, we designed FibeRobo with integrated interactivity. The material lends itself to a soft and quiet actuation with no additional hardware. Using our

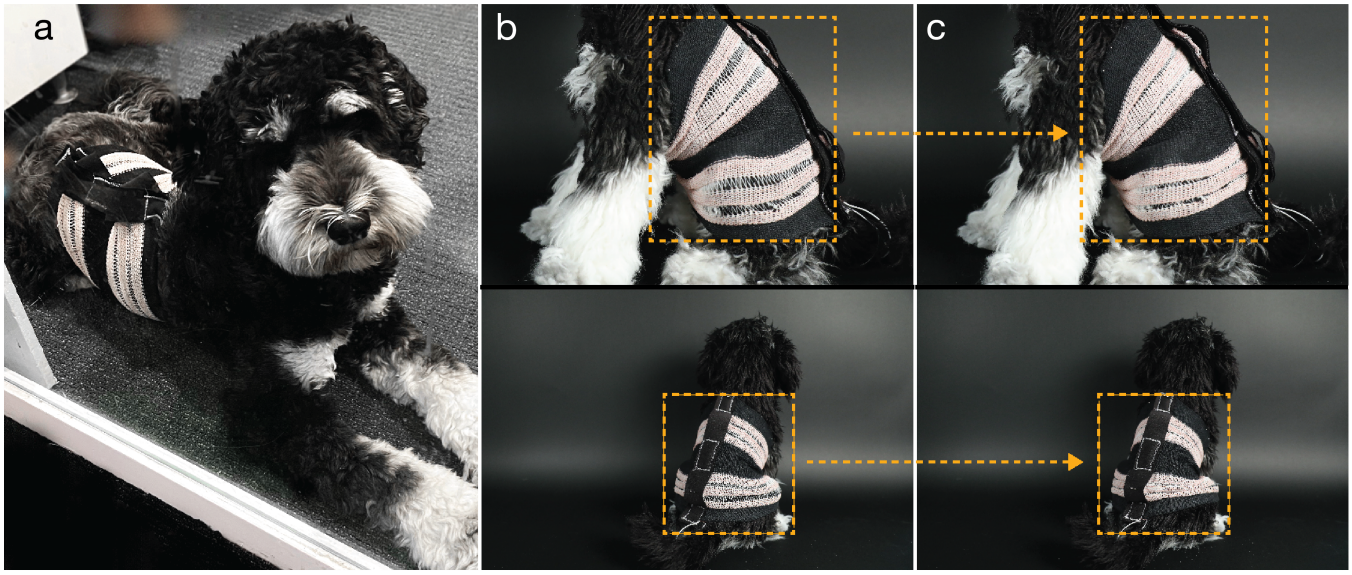

Figure 15: A tubular knitted dog jacket with an embedded heating element that provides thermal and mechanical feedback on the dog's torso for a calming hug. (a) a beautiful office dog, sadly watching authors prepare a paper submission; (b) a stuffed dog replica wearing the unactuated jacket state; (c) actuated form of the jacket tightened around the torso.

low-temperature fiber, we can produce a lightweight and thin compression garment that feels and looks like fabric. Because our fiber is machine knittable, a knitter could quickly produce the prototype.

In this scenario, the dog wears a loose, comfortable shirt. If the dog begins to whine or bark, the owner (usually outside the office doing lab work) can activate the vest through Bluetooth. An ESP32-controlled mosfet initiates 12V/2.5A battery heating through the litz wire. The vest then warms up and caresses the dog's torso, allowing the owner to 'send a hug' across the room. For documentation and ethical reasons, we demonstrate the prototype on a stuffed animal replica of the initially intended dog. The specific compression force does require testing and tuning to be effective but still comfortable. While this demo communicates the potential of FibeRobo as a digitally controlled affective wearable, future development will require user studies and calibration of the compression forces to prove effectivity while preserving comfort [9].

7.3.2 Knitting Development: Structure Search. Knit designers can control the local structure of a knitted object to produce variable stretchability and stiffness. Recent research has explored ways to design these properties into fully knitted objects [13, 14, 22]. With FibeRobo, we explored and achieved continuous jersey knit (Figure 16, a-d), horizontal inlay (Figure 16, e-f), and lace knit (Figure 16, g-h) techniques on a standard gauge 4.5mm flat-bed weft knitting machine (Brother KH940). The oil and powder coating on the fiber allows it to be appropriately tensioned and run smoothly on the yarn feeder mechanism. This simple and bio-safe post-processing significantly improves the fiber characteristics for withstanding tensions imposed by the yarn tensioning mechanism and the needles.

Another recent technique that attracted the interest of researchers is the "inlay" technique. Inlaying, called "knitweave," combines knitting and weaving by placing horizontal or vertical yarns between the stitches. We utilized this technique to increase contraction force parallel to the inlay direction and decrease stretchability on demand (Figure 16, c-d).

7.3.3 Knitting Development: Integration of Heating Element. Additionally, we explored the knitting of the LCE fiber with a non-elastic heating element, a silk-covered litz wire (Awg38, Rvyuan). We ran both threads through the same yarn carrier and knitted plain jersey fabric on a single bed. We quickly achieved a robust knit structure despite the different elasticities of the two fibers (Figure 17).

Figure 17a combines the lacing technique with five rows of jersey knit with litz wire and LCE fiber. The tubular fabric sample in Figure 17 used approximately 60 meters of continuous LCE fiber and 35 meters of continuous litz wire. Due to the large volume of continuous litz wire, the driving voltage requirements increased to 29V at 0.3A. Thus, we cut the litz wires to connect them in parallel to reduce the driving voltage, allowing localized control of the knit.

8 DISCUSSION

Textile interfaces are especially appealing because of the fabric's inherent tactile and programmable affordances. However, prior approaches to making interfaces out of textiles have focused on superimposing interactive elements (such as buttons, knobs, and sliders) onto fabric membranes. While these techniques succeed in making fabric interactive, the integration of rigid components such as stiff wires and motors often makes the fabric less fabric-like.

In this work, we take a material-centered bottom-up approach to provide textiles that are easier and more compatible with interaction design. Those designers, in turn, can create new types of fabric interfaces that leverage their deep understanding of the benefits,

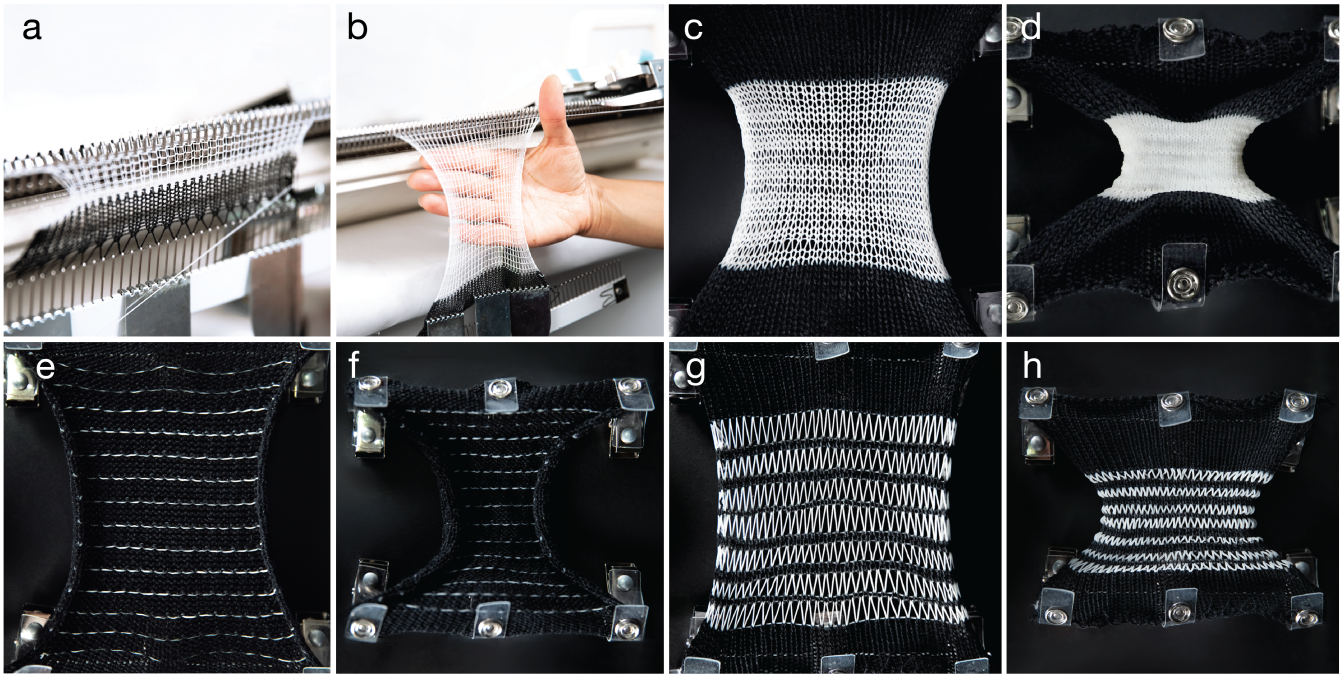

Figure 16: Knitted swatch with FibeRobo; (a) cast-on with black cotton yarn and every needle knit with Fiberobo, (b) finished jersey knit before cast-off, (c) single bed jersey knit with continuous LCE fiber initial state, (d) its thermally actuated state, (e) horizontal inlay knit LCE fiber initial state, (f) actuated state, (g) lace-knitted structure initial state, (h) actuated state.

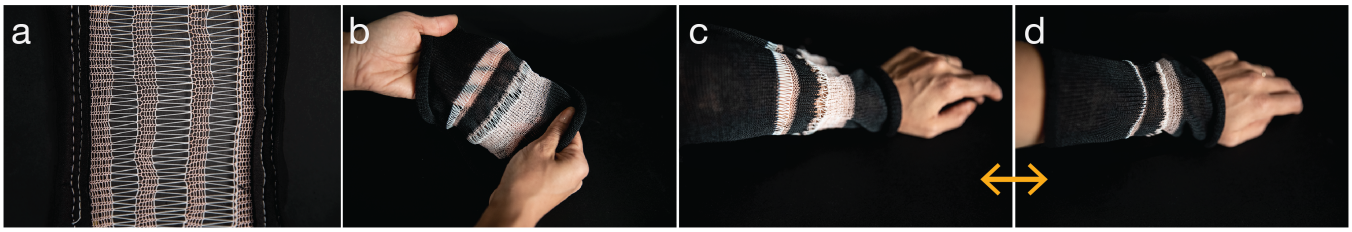

Figure 17: LCE knitted fabric with an additional heating element (a) A jersey knit fabric with five rows of LCE/litz and one long row of LCE pattern; (b) a tubular lace knitted fabric with embedded heating element for localized compression; (c) initial state o the sleeve when worn on the human arm; (d) actuated state of the sleeve with longitudinal contraction and subtle radial compression.

affordances, and structuring of fabric. This effort is motivated by the assumption that textile designers are already experts in designing interactive textiles but simply lack a tool well fit for their processes. For example, SMA is too stiff for machine knitting, requires manual post-processing for integration, and wears out quickly. On the other hand, an ideal interactive fiber is workable like any other fiber, incorporates sensing and heating elegantly, and is adaptable to different use cases. To achieve this, we informed the development of FibeRobo with the guiding principles of integrated interactivity, process compatibility, and modifiable materiality.

First, for FibeRobo to access the audience of people already skilled in textile design, the fiber needs to be able to leave the lab and enter the knitting machine. To be used like normal fibers, LCE fibers need to be long, even, thin, and flexible with sufficient mechanical strength for textile fabrication machinery. Doing so is nontrivial but led us to develop a DIY and minimal-cost desktop UV fiber drawing setup. With this system, hundreds of meters of machine-knittable fiber can be produced in a single day and handed off to the fabric designer. Through our experimentation and characterization of key parameters related to each fabrication approach, we provide a compass for these fabricators to engender their designs without starting from scratch.

The second principle is integrated interactivity. This principle led us to identify liquid crystal elastomers as promising due to their large contractions, skin safety, and self-reversibility. Our first step is creating a robust method for producing large volumes of even fiber. This method is a good place to start, but more is needed to be a toolkit for textile interfaces. Achieving interactivity required us

to integrate heating and sensing elements without compromising the affordances of a textile. To find the best solutions, we developed multiple techniques conducive to the specific fabrication approach (knitting, weaving, embroidery, braiding).

The third principle, and a key benefit of a bottom-up material approach, is Modifiable Materiality. The diameter of the fiber, and its thermal response speed, can be altered by changing the drawing parameters, such as the extrusion speed and nozzle size. By changing the composition of the precursor resin, one can lower the actuation temperature to enable body-temperature response. While we aimed to make FibeRobo as versatile as possible, we cannot predict and accommodate every use case. However, since external researchers would be making the fiber in-house, they possess an unrestricted ability to extend the design space on their own accord by customizing the precursor material.

9 FUTURE WORK AND LIMITATIONS

Despite our best efforts, the guiding principles could only sometimes be upheld. While aspects of modifiable materiality are synergistic with process compatibility (i.e., dying with carbon black, braiding), the ability to synthesize tailored polymers in a wet lab falls outside of most textile designer's skill sets. However, we still decided to include that process to make FibeRobo as versatile as possible for those who replicate the work. In the future, we can envision the commercialization of such LCE fibers, which removes the need for wet lab and machine building experience. In the meantime, this method is accessible to researchers with spaces equipped with a portable ductless fume hood or spray painting station with air filtration. We checked with our local EHS team that one could also build their own fume hood [43], assuming they also receive approval from their local EHS team.

Additionally, some technical limitations in liquid crystal elastomers impeded our ability to fulfill the guiding principles. For example, textile designers carefully consider the impact of fashion waste on pollution and landfills. In its current form, FibeRobo is not recyclable; however, emerging developments in biodegradable liquid crystal elastomers could ameliorate that [28]. In some cases, it was not the LCE fiber that inhibited compatibility but the conductive thread. We found the stretchable LCE fiber considerably more straightforward to work with during knitting than the commercially available conductive fibers due to their stiffness.

While we introduced some key techniques for integrated interactivity, there are still several relevant sensing techniques that we still need to employ. For example, future work could apply the pinch, grab, and hover detection developed by Olwal et al. in I/O Braid [24]. Similarly, while we demonstrate a set of actuating primitives for weaving, knitting, and embroidery, developing a morphing behavior taxonomy and a detailed exploration of the qualitative design space and implications remains an exciting design challenge. Through developing our illustrative applications, we began to address challenges regarding when and why fabric shape change should occur.

Finally, in section 3.2, we briefly mention craftsperson compatibility. This future goal is motivated by the observation that the textile craft community is already skilled in textile programming and could be ideal collaborators for inventing new interactive textiles. We hypothesize that the less you change their practices, the more they can leverage their years of experience. In this work, we focus purely on the mechanical compatibility of the fiber with unmodified textile tools. Moving forward, we want to paint a bigger picture that interweaves the textile tools and the people operating them through future workshops and investigations.

10 CONCLUSION

In this work, we present FibeRobo, a thermally-actuated liquid crystal elastomer (LCE) fiber that can be embedded or structured into textiles. FibeRobo exhibits three distinct properties that set it apart from other artificial muscles explored in HCI. First, FibeRobo is capable of rapid thermal self-reversing actuation with large displacements (~40%). Second, we present a reproducible UV fiber drawing setup that allows the production of hundreds of meters of fiber with a sub-millimeter diameter. Third, FibeRobo is fully compatible with existing textile manufacturing machinery such as weaving looms, embroidery machines, and knitting machines. We also provide a mechanical characterization of the fibers and demonstrate the ability to establish higher hierarchical textile structures. Finally, we introduce a set of applications that illustrate the design space enabled by FibeRobo, including a bra with dynamic support, a blooming lamp, and a canine compression garment. By providing a robust and manufacturing-minded actuating fiber system, FibeRobo has the potential to enable transformative textile tinkering to anyone with a sewing needle.

ACKNOWLEDGMENTS

The authors would like to acknowledge the support provided by the William Asbjornsen Albert Memorial Fellowship, Dr. Martin Luther King Jr. Visiting Professor Program, Toppan Printing Co., Ltd., Honda Research, Chinese Scholarship Council, Haystack Mountain School of Craft, and Shima Seiki. The author is grateful for Stefanie Mueller, Nadya Peek, Irmandy Wicaksono, Ken Nakagaki, and Leah Albaugh, who provided suggestions and guidance. The authors would also like to thank Elise O'Hara for her administrative assistance and Natalie Cardenas for early-stage sewing explorations. Last, the authors thank the first author's dog, Professor, for being a marvelous model and muse.

REFERENCES

[1] Ozgun Kilic Afsar, Ali Shtarbanov, Hila Mor, Ken Nakagaki, Jack Forman, Karen Modrei, Seung Hee Jeong, Klas Hjort, Kristina Hook, and Hiroshi Ishii. 2021. OmniFiber: Integrated Fluidic Fiber Actuators for Weaving Movement-based Interactions into the 'Fabric of Everyday Life.' In *34th Annual ACM Symposium on User Interface Software and Technology*. https://programs.sigchi.org/uist/2021/program/content/61366

[2] Aditya Agrawal, Huiying Chen, Hojin Kim, Bohan Zhu, Oluwatomiyin Adetiba, Andrea Miranda, Alin Cristian Chipara, Pulickel M. Ajayan, Jeffrey G. Jacot, and Rafael Verduzco. 2016. Electromechanically Responsive Liquid Crystal Elastomer Nanocomposites for Active Cell Culture. *ACS Macro Lett.* 5, 12 (December 2016), 1386–1390. https://doi.org/10.1021/acsmacrolett.6b00554

[3] Roland Aigner, Mira Alida Haberfellner, and Michael Haller. 2022. spaceR: Knitting Ready-Made, Tactile, and Highly Responsive Spacer-Fabric Force Sensors for Continuous Input. In *Proceedings of the 35th Annual ACM Symposium on User Interface Software and Technology* (UIST '22), 1–15. https://doi.org/10.1145/3526113.3545694

[4] Lea Albaugh, James McCann, Scott E. Hudson, and Lining Yao. 2021. Engineering Multifunctional Spacer Fabrics Through Machine Knitting. In *Proceedings of the*

2021 CHI Conference on Human Factors in Computing Systems (CHI '21), 1–12. https://doi.org/10.1145/3411764.3445564

[5] Leah Buechley, Mike Eisenberg, Jaime Catchen, and Ali Crockett. 2008. The LilyPad Arduino: using computational textiles to investigate engagement, aesthetics, and diversity in computer science education. In *Proceedings of the SIGCHI Conference on Human Factors in Computing Systems* (CHI '08), 423–432. https://doi.org/10.1145/1357054.1357123

[6] Alexandra Delazio, Ken Nakagaki, Roberta L. Klatzky, Scott E. Hudson, Jill Fain Lehman, and Alanson P. Sample. 2018. Force Jacket: Pneumatically-Actuated Jacket for Embodied Haptic Experiences. In *Proceedings of the 2018 CHI Conference on Human Factors in Computing Systems* (CHI '18), 1–12. https://doi.org/10.1145/3173574.3173894

[7] Laura Devendorf, Joanne Lo, Noura Howell, Jung Lin Lee, Nan-Wei Gong, M. Emre Karagozler, Shiho Fukuhara, Ivan Poupyrev, Eric Paulos, and Kimiko Ryokai. 2016. "I don't Want to Wear a Screen": Probing Perceptions of and Possibilities for Dynamic Displays on Clothing. In *Proceedings of the 2016 CHI Conference on Human Factors in Computing Systems* (CHI '16), 6028–6039. https://doi.org/10.1145/2858036.2858192

[8] Kristen L. Dorsey, Sonia F. Roberts, Jack Forman, and Hiroshi Ishii. 2022. Analysis of DefeXtiles: a 3D printed textile towards garments and accessories. *J. Micromechanics Microengineering* 32, 3 (February 2022), 034005. https://doi.org/10.1088/1361-6439/ac4fad

[9] Julia C. Duvall, Nicholas Schleif, Lucy E. Dunne, and Brad Holschuh. 2019. Dynamic Compression Garments for Sensory Processing Disorder Treatment Using Integrated Active Materials. *J. Med. Devices* 13, 2 (March 2019). https://doi.org/10.1115/1.4042599

[10] Jack Forman, Mustafa Doga Dogan, Hamilton Forsythe, and Hiroshi Ishii. 2020. DefeXtiles: 3D Printing Quasi-Woven Fabric via Under-Extrusion. In *Proceedings of the 33rd Annual ACM Symposium on User Interface Software and Technology* (UIST '20), 1222–1233. https://doi.org/10.1145/3379337.3415876

[11] Jack Forman, Taylor Tabb, Youngwook Do, Meng-Han Yeh, Adrian Galvin, and Lining Yao. 2019. ModiFiber: Two-Way Morphing Soft Thread Actuators for Tangible Interaction. In *Proceedings of the 2019 CHI Conference on Human Factors in Computing Systems*. Association for Computing Machinery, New York, NY, USA, 1–11. https://doi.org/10.1145/3290605.3300890

[12] Maas Goudswaard, Abel Abraham, Bruna Goveia da Rocha, Kristina Andersen, and Rong-Hao Liang. 2020. FabriClick: Interweaving Pushbuttons into Fabrics Using 3D Printing and Digital Embroidery. In *Proceedings of the 2020 ACM Designing Interactive Systems Conference* (DIS '20), 379–393. https://doi.org/10.1145/3357236.3395569

[13] Megan Hofmann, Lea Albaugh, Ticha Sethapakadi, Jessica Hodgins, Scott E. Hudson, James McCann, and Jennifer Mankoff. 2019. KnitPicking Textures: Programming and Modifying Complex Knitted Textures for Machine and Hand Knitting. In *Proceedings of the 32nd Annual ACM Symposium on User Interface Software and Technology* (UIST '19), 5–16. https://doi.org/10.1145/3332165.3347886

[14] Megan Hofmann, Jennifer Mankoff, and Scott E. Hudson. 2020. KnitGIST: A Programming Synthesis Toolkit for Generating Functional Machine-Knitting Textures. In *Proceedings of the 33rd Annual ACM Symposium on User Interface Software and Technology* (UIST '20), 1234–1247. https://doi.org/10.1145/3379337.3415590

[15] Jin Hee (Heather) Kim, Kunpeng Huang, Simone White, Melissa Conroy, and Cindy Hsin-Liu Kao. 2021. KnitDermis: Fabricating Tactile On-Body Interfaces Through Machine Knitting. In *Designing Interactive Systems Conference 2021*, 1183–1200. https://doi.org/10.1145/3461778.3462007

[16] Jin Hee (Heather) Kim, Shreyas Dilip Patil, Sarina Matson, Melissa Conroy, and Cindy Hsin-Liu Kao. 2022. KnitSkin: Machine-Knitted Scaled Skin for Locomotion. In *Proceedings of the 2022 CHI Conference on Human Factors in Computing Systems* (CHI '22), 1–15. https://doi.org/10.1145/3491102.3502142

[17] Camille King, Laurie Buffington, Thomas J. Smith, and Temple Grandin. 2014. The effect of a pressure wrap (ThunderShirt®) on heart rate and behavior in canines diagnosed with anxiety disorder. *J. Vet. Behav.* 9, 5 (September 2014), 215–221. https://doi.org/10.1016/j.jveb.2014.06.007

[18] Xueyan Lin, Mohand O. Saed, and Eugene M. Terentjev. 2021. Continuous spinning aligned liquid crystal elastomer fibers with a 3D printer setup. *Soft Matter* 17, 21 (2021), 5436–5443. https://doi.org/10.1039/D1SM00432H

[19] Yiyue Luo, Kui Wu, Tomás Palacios, and Wojciech Matusik. 2021. KnitUI: Fabricating Interactive and Sensing Textiles with Machine Knitting. In *Proceedings of the 2021 CHI Conference on Human Factors in Computing Systems* (CHI '21), 1–12. https://doi.org/10.1145/3411764.3445780

[20] Yiyue Luo, Kui Wu, Andrew Spielberg, Michael Foshey, Daniela Rus, Tomás Palacios, and Wojciech Matusik. 2022. Digital Fabrication of Pneumatic Actuators with Integrated Sensing by Machine Knitting. In *Proceedings of the 2022 CHI Conference on Human Factors in Computing Systems* (CHI '22), 1–13. https://doi.org/10.1145/3491102.3517577

[21] Hua Ma and Junichi Yamaoka. 2022. SenSequins: Smart Textile Using 3D Printed Conductive Sequins. In *Proceedings of the 35th Annual ACM Symposium on User Interface Software and Technology* (UIST '22), 1–13. https://doi.org/10.1145/3526113.3545688

[22] Vidya Narayanan, Kui Wu, Cem Yuksel, and James McCann. 2019. Visual knitting machine programming. *ACM Trans. Graph.* 38, 4 (July 2019), 63:1-63:13. https://doi.org/10.1145/3306346.3322995

[23] Takahashi Nobuhiro, Okazaki Ryuta, Okabe Hiroyuki, Yoshikawa Hiromi, Aou Kanako, Yamakawa Shumpei, Yokoyama Maki, and K. Hiroyuki. 2011. Sense-Roid: Emotional Haptic Communication with Yourself. https://www.semanticscholar.org/paper/Sense-Roid-%3A-Emotional-Haptic-Communication-with-Nobuhiro-Ryuta/f839f0fd763ff25fae28e8f05e54f37edf485c0c

[24] Alex Olwal, Jon Moeller, Greg Priest-Dorman, Thad Starner, and Ben Carroll. 2018. I/O Braid: Scalable Touch-Sensitive Lighted Cords Using Spiraling, Repeating Sensing Textiles and Fiber Optics. In *Proceedings of the 31st Annual ACM Symposium on User Interface Software and Technology* (UIST '18), 485–497. https://doi.org/10.1145/3242587.3242638

[25] Huaishu Peng, Scott Hudson, Jennifer Mankoff, and James McCann. 2016. Soft printing with fabric. *XRDS Crossroads ACM Mag. Stud.* 22, 3 (April 2016), 50–53. https://doi.org/10.1145/2893499

[26] Huaishu Peng, Jennifer Mankoff, Scott E. Hudson, and James McCann. 2015. A Layered Fabric 3D Printer for Soft Interactive Objects. In *Proceedings of the 33rd Annual ACM Conference on Human Factors in Computing Systems* (CHI '15), 1789–1798. https://doi.org/10.1145/2702123.2702327

[27] Thomas Preindl, Cedric Honnet, Andreas Pointner, Roland Aigner, Joseph A. Paradiso, and Michael Haller. 2020. Sonoflex: Embroidered Speakers Without Permanent Magnets. In *Proceedings of the 33rd Annual ACM Symposium on User Interface Software and Technology* (UIST '20), 675–685. https://doi.org/10.1145/3379337.3415888

[28] Marianne E. Prévôt, Senay Ustunel, and Elda Hegmann. 2018. Liquid Crystal Elastomers—A Path to Biocompatible and Biodegradable 3D-LCE Scaffolds for Tissue Regeneration. *Materials* 11, 3 (March 2018), 377. https://doi.org/10.3390/ma11030377

[29] Michael L. Rivera, Jack Forman, Scott E. Hudson, and Lining Yao. 2020. Hydrogel-Textile Composites: Actuators for Shape-Changing Interfaces. In *Extended Abstracts of the 2020 CHI Conference on Human Factors in Computing Systems* (CHI EA '20), 1–9. https://doi.org/10.1145/3334480.3382788

[30] Michael L. Rivera, Melissa Moukperian, Daniel Ashbrook, Jennifer Mankoff, and Scott E. Hudson. 2017. Stretching the Bounds of 3D Printing with Embedded Textiles. In *Proceedings of the 2017 CHI Conference on Human Factors in Computing Systems* (CHI '17), 497–508. https://doi.org/10.1145/3025453.3025460

[31] Devin J. Roach, Chao Yuan, Xiao Kuang, Vincent Chi-Fung Li, Peter Blake, Marta Lechuga Romero, Irene Hammel, Kai Yu, and H. Jerry Qi. 2019. Long Liquid Crystal Elastomer Fibers with Large Reversible Actuation Strains for Smart Textiles and Artificial Muscles. *ACS Appl. Mater. Interfaces* 11, 21 (May 2019), 19514–19521. https://doi.org/10.1021/acsami.9b04401

[32] Mohand O. Saed, Cedric P. Ambulo, Hyun Kim, Rohit De, Vyom Raval, Kyle Searles, Danyal A. Siddiqui, John Michael O. Cue, Mihaela C. Stefan, M. Ravi Shankar, and Taylor H. Ware. 2019. Molecularly-Engineered, 4D-Printed Liquid Crystal Elastomer Actuators. *Adv. Funct. Mater.* 29, 3 (2019), 1806412. https://doi.org/10.1002/adfm.201806412

[33] Rajib K. Shaha, Daniel R. Merkel, Mitchell P. Anderson, Emily J. Devereaux, Ravi R. Patel, Amir H. Torbati, Nick Willett, Christopher M. Yakacki, and Carl P. Frick. 2020. Biocompatible liquid-crystal elastomers mimic the intervertebral disc. *J. Mech. Behav. Biomed. Mater.* 107, (July 2020), 103757. https://doi.org/10.1016/j.jmbbm.2020.103757

[34] Pedro E. S. Silva, Xueyan Lin, Maija Vaara, Mithila Mohan, Jaana Vapaavuori, and Eugene M. Terentjev. Active Textile Fabrics from Weaving Liquid Crystalline Elastomer Filaments. *Adv. Mater.* n/a, n/a , 2210689. https://doi.org/10.1002/adma.202210689

[35] Haruki Takahashi and Jeeeun Kim. 2019. 3D Printed Fabric: Techniques for Design and 3D Weaving Programmable Textiles. In *Proceedings of the 32nd Annual ACM Symposium on User Interface Software and Technology* (UIST '19), 43–51. https://doi.org/10.1145/3332165.3347896

[36] James Keng Soon Teh, Adrian David Cheok, Roshan L. Peiris, Yongsoon Choi, Vuong Thuong, and Sha Lai. 2008. Huggy Pajama: a mobile parent and child hugging communication system. In *Proceedings of the 7th international conference on Interaction design and children* (IDC '08), 250–257. https://doi.org/10.1145/1463689.1463763

[37] Thingiverse.com. 3D printed braiding machine by Fraens. https://www.thingiverse.com/thing:5355407

[38] Te-Yen Wu, Lu Tan, Yuji Zhang, Teddy Seyed, and Xing-Dong Yang. 2020. Capacitivo: Contact-Based Object Recognition on Interactive Fabrics using Capacitive Sensing. In *Proceedings of the 33rd Annual ACM Symposium on User Interface Software and Technology* (UIST '20), 649–661. https://doi.org/10.1145/3379337.3415829

[39] C. M. Yakacki, M. Saed, D. P. Nair, T. Gong, S. M. Reed, and C. N. Bowman. 2015. Tailorable and programmable liquid-crystalline elastomers using a two-stage thiol–acrylate reaction. *RSC Adv.* 5, 25 (February 2015), 18997–19001. https://doi.org/10.1039/C5RA01039J

[40] Willa Yunqi Yang, Yumeng Zhuang, Luke Andre Darcy, Grace Liu, and Alexandra Ion. 2022. Reconfigurable Elastic Metamaterials. In *Proceedings of the 35th Annual ACM Symposium on User Interface Software and Technology* (UIST '22), 1–13.

https://doi.org/10.1145/3526113.3545649
[41] Jingwen Zhu and Hsin-Liu (Cindy) Kao. 2022. Scaling E-Textile Production: Understanding the Challenges of Soft Wearable Production for Individual Creators. In *Proceedings of the 2022 ACM International Symposium on Wearable Computers* (ISWC '22), 94–99. https://doi.org/10.1145/3544794.3558475
[42] 2022. PEmbroider. https://github.com/CreativeInquiry/PEmbroider
[43] 2022. DIY Fume Hood. *Make: DIY Projects and Ideas for Makers*. https://makezine.com/projects/diy-fume-hood/
[44] DYNALLOY, Inc. Makers of Dynamic Alloys. https://www.dynalloy.com/flexinol_70_90.php
[45] Environmental Health & Safety: Occupational Safety: UV Light Guidelines. https://www.safety.rochester.edu/ih/uvlight.html

A APPENDICES

A SYNTHESIS GUIDELINES

All measurements for the synthesis can be performed with an analytical balance. However, micropipettes are helpful for liquid volumes. Generally, the synthesis accommodates minor measurement errors; however, errors should still be avoided as they may reduce the contraction length or require slight spinning parameter adjustment. In our experience, minor measurement errors never caused the resin synthesis to fail, but four main errors did cause complete failure. These are: overheating the resin (causing it to crystallize irreversibly), leaving the photoinitiator or final resin in the light during storage (causing the resin to cure prematurely), allowing the resin to cool before adding the initiator (making homogenous mixing impossible due to the high viscosity) and waiting too long (>1 week, but ideally within 24 hours) between preparing the resin and spinning the fiber (resulting in a hardened resin or a weak fiber).

B SYNTHESIS MATERIALS

- **RM82** (1,4-Bis-[4-(6-acryloyloxyhexyloxy)benzoyloxy]-2-methylbenzene): A reactive liquid crystal compound known as mesogens
- **RM257** (Bis-[4-(3-acryloyloxypropyloxy)benzoyloxy]-2-methylbenzene): A reactive mesogen that can be combined with RM82 to lower the actuation temperature
- **EDDET** (2,2-(ethylenedioxy)diethanethiol): A joining molecule that links mesogens together into elongated chains
- **GDMP** (glycol di(3-mercaptopropionate)): A joining molecule that is used in place of EDDET for lower-temperature actuating fibers
- **TATATO** (1,3,5-triallyl-1,3,5-triazine-2,4,6(1H,3H,5H)-trione): A common vinyl crosslinker that connects the chains to form an elastic network. Note: TATATO may arrive as a solid but can be melted in a lukewarm water bath to allow more straightforward measurement via pipette.
- **DPA** (Dipropylamine): A chemical initiator that catalyzes the first reaction where mesogens are linked into long chains resulting in a viscous resin that can be extruded and drawn.
- **I-651** (2,2-dimethoxy-2-phenylacetophenone): A photoinitiator that, when exposed to UV (365nm) light, starts the second reaction where TATATO binds the chains together, solidifying the fiber. Note: the photoinitiator must be stored in a dark area to avoid premature initiation.
- **BHT** (Butylated hydroxytoluene): A reaction inhibitor that extends the shelf life of the resin.

EDDET, TATATO, BHT, I-651, and DPA were purchased from Sigma Aldrich. GDMP was purchased from Fisher Scientific. RM82 and RM257 were purchased in small quantities from Sigma Aldrich and bulk from Daken Chemical.